# *Parity Proofs of the Bell-Kochen-Specker Theorem Based on the 600-cell*

**Foundations of Physics**
An International Journal
Devoted to the Conceptual
Bases and Fundamental
Theories of Modern Physics

ISSN 0015-9018
Volume 41
Number 5

Found Phys (2011) 41:883-904
DOI 10.1007/
s10701-011-9534-7

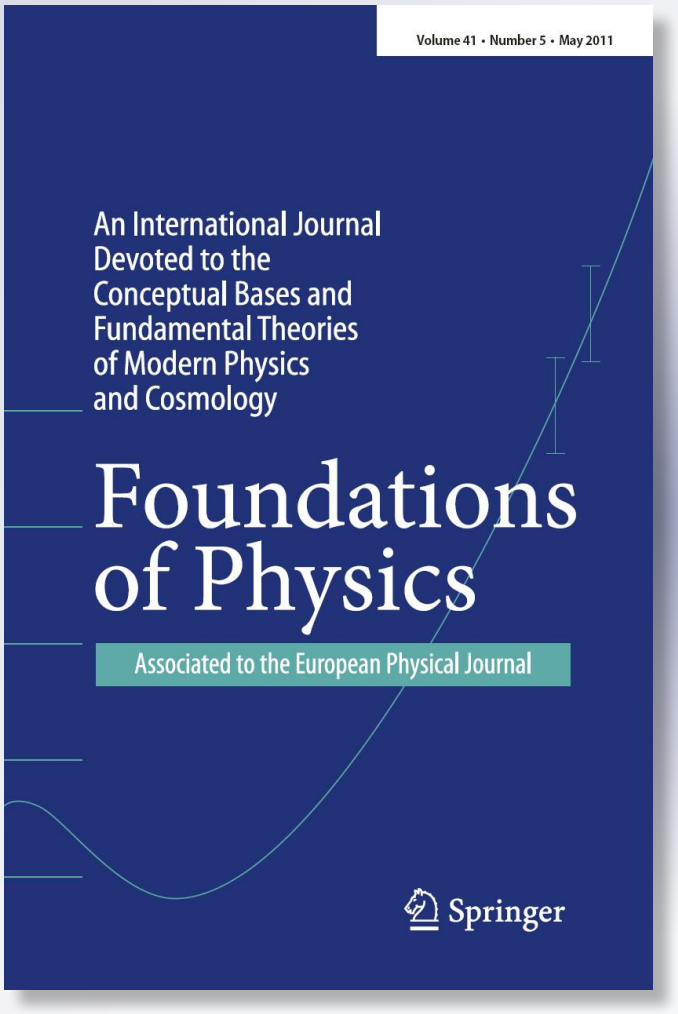


Springer

Found Phys (2011) 41: 883–904
DOI 10.1007/s10701-011-9534-7

# Parity Proofs of the Bell-Kochen-Specker Theorem Based on the 600-cell

**Mordecai Waegell · P.K. Aravind · Norman D. Megill · Mladen Pavičić**

Received: 21 October 2010 / Accepted: 4 January 2011 / Published online: 15 January 2011


**Abstract** The set of 60 real rays in four dimensions derived from the vertices of a 600-cell is shown to possess numerous subsets of rays and bases that provide basis-critical parity proofs of the Bell-Kochen-Specker (BKS) theorem (a basis-critical proof is one that fails if even a single basis is deleted from it). The proofs vary considerably in size, with the smallest having 26 rays and 13 bases and the largest 60 rays and 41 bases. There are at least 90 basic types of proofs, with each coming in a number of geometrically distinct varieties. The replicas of all the proofs under the symmetries of the 600-cell yield a total of almost a hundred million parity proofs of the BKS theorem. The proofs are all very transparent and take no more than simple counting to verify. A few of the proofs are exhibited, both in tabular form as well as in the form of MMP hypergraphs that assist in their visualization. A survey of the proofs is given, simple procedures for generating some of them are described and their applications are discussed. It is shown that all four-dimensional parity proofs of the BKS theorem can be turned into experimental disproofs of noncontextuality.

M. Waegell · P.K. Aravind (✉)
Physics Department, Worcester Polytechnic Institute, Worcester, MA 01609, USA
e-mail: paravind@wpi.edu

M. Waegell
e-mail: caiw@wpi.edu

N.D. Megill
Boston Information Group, 19 Locke Ln., Lexington, MA 02420, USA

M. Pavičić
Institute for Theoretical Atomic, Molecular and Optical Physics at Physics Department at Harvard University and Harvard-Smithsonian Center for Astrophysics, Cambridge, MA 02138, USA
e-mail: mpavicic@grad.hr

M. Pavičić
Chair of Physics, Faculty of Civil Engineering, University of Zagreb, Zagreb, Croatia

**Keywords** Bell-Kochen-Specker theorem · 600-cell · Quantum noncontextuality · Quantum cryptography

## 1 Introduction

In a recent paper ([1], the suggestion that the 600-cell could be used to prove the BKS theorem was first made in [39]) two of us showed that the system of 60 rays derived from the vertices of a 600-cell could be used to give two new proofs of the Bell-Kochen-Specker (BKS) theorem [2, 3] ruling out the existence of noncontextual hidden variables theories. A later work [4] presented several additional proofs based on the same set of rays. The purpose of this paper is to add to the store of proofs in [4], but, even more than that, to convey a feeling for the variety and flavor of the proofs (both through the examples presented here and the far more extensive listing on the website[1]) and to show interested readers how many of the proofs can be obtained by simple constructions based on the geometry of the 600-cell. There are two aspects of the present proofs that make them noteworthy. The first is that they are all "parity proofs" (this term is explained in Sect. 2) whose validity can be checked by simple counting. And the second is that there are about a hundred million of them in this 60-ray system. While many of the proofs are just replicas of each other under the symmetries of the 600-cell, the number of distinct proofs, in terms of size and other characteristics, is still fairly large (we used a random exhaustive generation of proofs to obtain over 8,000 proofs, most of which turned out to be parity proofs [5]). The sheer profusion and variety of parity proofs contained in the 600-cell is unmatched by that in any other system we are aware of and motivated us to study this system in detail, both for its geometric interest as well as for its possible applications.

A brief survey of earlier proofs of the BKS theorem may be helpful in setting the present work in context. After Kochen and Specker [3] first gave a finitary proof of their theorem using 117 directions in ordinary three-dimensional space, a number of authors gave alternative proofs in three [6–10], four [6, 11–17] and higher [18–21] dimensions. Some of the proofs in higher dimensions are much simpler than the three-dimensional proofs and, in fact, are examples of the "parity proofs" we discuss throughout this paper. In recent years there has been a resurgence of interest in the BKS theorem as a result of the fruitful suggestion by Cabello [22, 23] of how it might be experimentally tested. Cabello's basic observation is that many proof of the BKS theorem based on a finite set of rays and bases can be converted into an inequality that must be obeyed by a noncontextual hidden variables theory but is violated by quantum mechanics. Experimental tests of Cabello-like inequalities have been carried out in four-level systems realized by ions [24], neutrons [25], photons [26] and nuclear spins [27], and violations of the inequalities have been observed in all the cases. Still other inequalities, some state-dependent and others not, that must be satisfied by noncontextual theories have been derived for qutrits [28], n-qubit systems [29]

[1] http://users.wpi.edu/~paravind/BKS600-cellDisplay.html (this site has a link to an excel file that lists many examples of the parity proofs in Table 3 and also a link to a Web Application that shows many of these proofs in an easily visualized tabular form).

and hypergraph models [30]. It has been argued in [31] that contextuality is the key feature underlying quantum nonlocality. A wide ranging discussion of the Kochen-Specker and other no-go theorems, as well as the subtle interplay between the notions of contextuality, nonlocality and complementarity, can be found in [32]. Aside from their foundational interest, proofs of the BKS theorem are useful in connection with protocols such as quantum cryptography [33], random number generation [34] and parity oblivious transfer [35].

This paper is organized as follows. Section 2 reviews the BKS theorem and explains what is meant by a "parity proof" of it. An explanation is also given of the notion of a "basis-critical" parity proof, since only such proofs are presented in this paper. Section 3 introduces the system of 60 rays and 75 bases derived from the 600-cell that is the source of all the proofs presented in this paper. A notation is introduced for the ray-basis sets underlying the parity proofs, and an overview is given of all the parity proofs we were able to find in the 600-cell. The algorithm we used to search for the proofs is described, and a few of the proofs are displayed in a tabular form so that the reader can see how they work. An equivalent McKay-Megill-Pavicic (MMP) hypergraph representation [4, 15, 36] is used to give the reader a graphical visualization of some of the proofs. In an MMP hypergraph vertices correspond to rays and edges to tetrads of mutually orthogonal rays (see Figs. 1 and 2). Section 4 summarizes the general features of the parity proofs and also points out their relevance for quantum key distribution and experimental disproofs of noncontextuality. The Appendix reviews some basic geometrical facts about the 600-cell and shows how they can be used to give simple constructions for some of the parity proofs in Table 3. Space prevents us from discussing more than a handful of examples, but the ones chosen may help to convey some feeling for the rest. Some virtues of the treatment in the Appendix are (a) that it allows many of the proofs to be constructed "by hand" without the need to look up a compilation, (b) that it allows the number of replicas of a particular proof under the symmetries of the 600-cell to be determined, and (c) that it reveals close connections between different proofs that might otherwise appear to be unrelated. However the treatment in the Appendix is not needed for an understanding of the main results of this paper and can be omitted by those not interested in it.

This paper is written to be self-contained and can be read without any knowledge of our earlier work [1, 4] on this problem.

## 2 Parity Proofs of the BKS Theorem; Basis Critical Sets

The BKS theorem asserts that in any Hilbert space of dimension $d \geq 3$ it is always possible to find a finite set of rays[2] that cannot each be assigned the value 0 or 1 in

[2]We explain some aspects of our terminology for readers unfamiliar with the BKS theorem. By a "ray" we mean an equivalence class of quantum states that differ from each other only by an overall phase. Only orthogonalities between states play a role in the BKS theorem, and since orthogonalities are unaffected by a change of phase, it is rays rather than states that are of relevance for the BKS theorem. The bases are related to the projective measurements that one can carry out on the system. The projectors on to the rays in a basis form a set of commuting operators, and a joint measurement of these projectors causes the system to collapse into the ray associated with one of them, with the eigenvalue 1 being returned for

such a way that (i) no two orthogonal rays are both assigned the value 1, and (ii) not all members of a basis, i.e. a set of $d$ mutually orthogonal rays, are assigned the value 0. The proof of the theorem becomes trivial if one can find a set of $R$ rays in $d$ dimensions that form an odd number, $B$, of bases in such a way that each ray occurs an even number of times among those bases. Then the assignment of 0's and 1's to the rays in accordance with rules (i) and (ii) is seen to be impossible because the total number of 1's over all the bases is required to be both odd (because each basis must have exactly one ray labeled 1 in it) and even (because each ray labeled 1 is repeated an even number of times). Any set of $R$ rays and $B$ bases that gives this even-odd contradiction furnishes what we call a "parity proof" of the BKS theorem.

Let us denote a set of $R$ rays that forms $B$ bases a $R$-$B$ set. A $R$-$B$ set that yields a parity proof of the BKS theorem will be said to be basis-critical (or simply critical) if dropping even a single basis from it causes the BKS proof to fail. Basis-criticality is not to be confused with ray-criticality, which takes all orthogonalities between rays into account and not just those in the limited set of bases considered. We focus on basis-criticality because it is more relevant to experimental tests of the Kochen-Specker theorem. Such tests typically involve projective measurements that pick out whole sets of bases, and performing a test that corresponds to a basis-critical set is an efficient strategy because it involves no superfluous measurements. The only parity proofs exhibited in this paper are those that correspond to basis-critical sets.

## 3 Overview of Parity Proofs Contained in the 600-cell

Table 1 shows the 60 rays derived from the vertices of the 600-cell and Table 2 the 75 bases (of four rays each) formed by them. Each ray occurs in exactly five bases, with its 15 companions in these bases being the only other rays it is orthogonal to. Thus Table 2 (or the "basis table") captures all the orthogonalities between the rays and is completely equivalent to their Kochen-Specker diagram.

The rays and bases of the 600-cell make up a 60-75 set ( i.e., one with 60 rays and 75 bases). This set does not give a parity proof, but contains a large number of subsets that do. A $R$-$B$ subset of the 60-75 set that yields a parity proof must have each of its rays occur either twice or four times among its bases (these being the only possibilities for the 600-cell). It is easy to see that the number of rays that occur four times is $2B - R$, while the number that occur twice is $2R - 2B$.

Table 3 gives an overview of all the parity proofs we have found in the 600-cell. The smallest proof is provided by a 26-13 set (in which all 26 rays occur twice each among the bases) and the largest by a 60-41 set (in which 38 rays occur twice each and 22 rays four times each among the bases). Moving one step to the left in any row of Table 3 causes the number of rays that occur four times to go up by one and the number that occur twice to go down by two.

this projector and 0 for the others. This explains why a hidden variables theory attempting to simulate quantum mechanics is required to assign a 1 to one projector and 0's to the others. The rays and bases in our theoretical discussion correspond to states and compatible sets of projective measurements in an actual experiment.

**Table 1** The 60 rays of the 600-cell. The numbers following each ray are its components in an orthonormal basis, with $\tau = (1+\sqrt{5})/2$, $\kappa = 1/\tau$, a bar over a number indicating its negative and commas being omitted between components. The entries can also be regarded as coordinates of 60 of the vertices of a 600-cell, located on a sphere of radius 2 centered at the origin. The other 60 vertices are the antipodes of these

| | | | |
|---|---|---|---|
| $1 = 2000$ | $2 = 0200$ | $3 = 0020$ | $4 = 0002$ |
| $5 = 1111$ | $6 = 11\overline{1}\overline{1}$ | $7 = 1\overline{1}1\overline{1}$ | $8 = 1\overline{1}\overline{1}1$ |
| $9 = 1\overline{1}\overline{1}\overline{1}$ | $10 = 1\overline{1}11$ | $11 = 11\overline{1}1$ | $12 = 111\overline{1}$ |
| $13 = \kappa 0\overline{\tau}\overline{1}$ | $14 = 0\kappa 1\overline{\tau}$ | $15 = \tau\overline{1}\kappa 0$ | $16 = 1\tau 0\kappa$ |
| $17 = \tau\kappa 0\overline{1}$ | $18 = 10\kappa\tau$ | $19 = \kappa\overline{\tau}\overline{1}0$ | $20 = 01\overline{\tau}\kappa$ |
| $21 = 1\kappa\tau 0$ | $22 = \tau 0\overline{1}\kappa$ | $23 = 0\tau\overline{\kappa}\overline{1}$ | $24 = \kappa\overline{1}0\overline{\tau}$ |
| $25 = \tau 01\kappa$ | $26 = 0\tau\overline{\kappa}1$ | $27 = 1\overline{\kappa}\tau 0$ | $28 = \kappa 10\overline{\tau}$ |
| $29 = 0\kappa 1\tau$ | $30 = \tau 1\overline{\kappa}0$ | $31 = \kappa 0\tau\overline{1}$ | $32 = 1\overline{\tau}0\kappa$ |
| $33 = \tau\overline{\kappa}0\overline{1}$ | $34 = 01\overline{\tau}\overline{\kappa}$ | $35 = 10\overline{\kappa}\tau$ | $36 = \kappa\tau 10$ |
| $37 = \tau 0\overline{1}\overline{\kappa}$ | $38 = 0\tau\kappa\overline{1}$ | $39 = 1\overline{\kappa}\tau 0$ | $40 = \kappa 10\tau$ |
| $41 = \tau 1\kappa 0$ | $42 = 0\kappa\overline{1}\overline{\tau}$ | $43 = 1\overline{\tau}0\overline{\kappa}$ | $44 = \kappa 0\overline{\tau}1$ |
| $45 = 01\tau\kappa$ | $46 = \tau\overline{\kappa}01$ | $47 = \kappa\tau\overline{1}0$ | $48 = 10\kappa\overline{\tau}$ |
| $49 = \kappa 0\tau 1$ | $50 = 0\kappa\overline{1}\tau$ | $51 = \tau\overline{1}\overline{\kappa}0$ | $52 = 1\tau 0\overline{\kappa}$ |
| $53 = 10\overline{\kappa\tau}$ | $54 = \tau\kappa 01$ | $55 = 01\tau\overline{\kappa}$ | $56 = \kappa\overline{\tau}10$ |
| $57 = \tau 01\overline{\kappa}$ | $58 = 1\kappa\overline{\tau}0$ | $59 = \kappa\overline{1}0\tau$ | $60 = 0\tau\kappa 1$ |

**Table 2** The 75 bases formed by the 60 rays of the 600-cell, with the rays numbered as in Table 1

| | A | | | | B | | | | C | | | | D | | | | E | | | |
|---|---|---|---|---|---|---|---|---|---|---|---|---|---|---|---|---|---|---|---|---|
| A′ | 1 | 2 | 3 | 4 | 31 | 42 | 51 | 16 | 22 | 60 | 39 | 28 | 57 | 23 | 27 | 40 | 44 | 29 | 15 | 52 |
| | 5 | 6 | 7 | 8 | 38 | 24 | 58 | 25 | 18 | 47 | 33 | 55 | 36 | 53 | 20 | 46 | 59 | 26 | 37 | 21 |
| | 9 | 10 | 11 | 12 | 56 | 45 | 17 | 35 | 13 | 32 | 50 | 41 | 43 | 49 | 30 | 14 | 34 | 19 | 48 | 54 |
| B′ | 13 | 14 | 15 | 16 | 43 | 54 | 3 | 28 | 34 | 12 | 51 | 40 | 9 | 35 | 39 | 52 | 56 | 41 | 27 | 4 |
| | 17 | 18 | 19 | 20 | 50 | 36 | 10 | 37 | 30 | 59 | 45 | 7 | 48 | 5 | 32 | 58 | 11 | 38 | 49 | 33 |
| | 21 | 22 | 23 | 24 | 8 | 57 | 29 | 47 | 25 | 44 | 2 | 53 | 55 | 1 | 42 | 26 | 46 | 31 | 60 | 6 |
| C′ | 25 | 26 | 27 | 28 | 55 | 6 | 15 | 40 | 46 | 24 | 3 | 52 | 21 | 47 | 51 | 4 | 8 | 53 | 39 | 16 |
| | 29 | 30 | 31 | 32 | 2 | 48 | 22 | 49 | 42 | 11 | 57 | 19 | 60 | 17 | 44 | 10 | 23 | 50 | 1 | 45 |
| | 33 | 34 | 35 | 36 | 20 | 9 | 41 | 59 | 37 | 56 | 14 | 5 | 7 | 13 | 54 | 38 | 58 | 43 | 12 | 18 |
| D′ | 37 | 38 | 39 | 40 | 7 | 18 | 27 | 52 | 58 | 36 | 15 | 4 | 33 | 59 | 3 | 16 | 20 | 5 | 51 | 28 |
| | 41 | 42 | 43 | 44 | 14 | 60 | 34 | 1 | 54 | 23 | 9 | 31 | 12 | 29 | 56 | 22 | 35 | 2 | 13 | 57 |
| | 45 | 46 | 47 | 48 | 32 | 21 | 53 | 11 | 49 | 8 | 26 | 17 | 19 | 25 | 6 | 50 | 10 | 55 | 24 | 30 |
| E′ | 49 | 50 | 51 | 52 | 19 | 30 | 39 | 4 | 10 | 48 | 27 | 16 | 45 | 11 | 15 | 28 | 32 | 17 | 3 | 40 |
| | 53 | 54 | 55 | 56 | 26 | 12 | 46 | 13 | 6 | 35 | 21 | 43 | 24 | 41 | 8 | 34 | 47 | 14 | 25 | 9 |
| | 57 | 58 | 59 | 60 | 44 | 33 | 5 | 23 | 1 | 20 | 38 | 29 | 31 | 37 | 18 | 2 | 22 | 7 | 36 | 42 |

Most of the sets in Table 3 were discovered through a computer search. The search algorithm is exhaustive, and quite simple: it starts from an arbitrary basis in Table 2 and adds one basis at a time in an attempt to obtain a target parity proof, $R$-$B$. Because every ray must appear two or four times in the proof, a ray appearing once or thrice among the bases already chosen is selected, and one of the (at most four) other bases containing that ray is added to the proof at each iteration. The algorithm explores all these possible bases-choices in a branching fashion, and saves computational time by skipping all branches in which the target $R$ is exceeded before $B$ bases have been

**Table 3** Overview of basis-critical parity proofs in the 600-cell. Each row shows all the $R$-$B$ parity proofs for a fixed value of $B$ and variable $R$ ($R$ = number of rays, $B$ = number of bases)

| B | R | | | | | | | | | | |
|---|---|---|---|---|---|---|---|---|---|---|---|
| 13 | 26 | | | | | | | | | | |
| 15 | 30 | | | | | | | | | | |
| 17 | 32 | 33 | 34 | | | | | | | | |
| 19 | 36 | 37 | 38 | | | | | | | | |
| 21 | 38 | 39 | 40 | 41 | 42 | | | | | | |
| 23 | 40 | 41 | 42 | 43 | 44 | 45 | 46 | | | | |
| 25 | 42 | 43 | 44 | 45 | 46 | 47 | 48 | 49 | 50 | | |
| 27 | 44 | 45 | 46 | 47 | 48 | 49 | 50 | 51 | 52 | 53 | 54 |
| 29 | 46 | 47 | 48 | 49 | 50 | 51 | 52 | 53 | 54 | 55 | 56 |
| 31 | 48 | 49 | 50 | 51 | 52 | 53 | 54 | 55 | 56 | 57 | 58 |
| 33 | 51 | 52 | 53 | 54 | 55 | 56 | 57 | 58 | 59 | 60 | |
| 35 | 53 | 54 | 55 | 56 | 57 | 58 | 59 | 60 | | | |
| 37 | 55 | 56 | 57 | 58 | 59 | 60 | | | | | |
| 39 | 58 | 59 | 60 | | | | | | | | |
| 41 | 60 | | | | | | | | | | |

chosen or those in which more than $2B - R$ rays appear three or four times or those in which any ray appears five times. This ensures that the search is exhaustive, and keeps the number of necessary iterations well below the upper bound of $4^B$. If any branch leads to a $R$-$B$ set, then it is necessarily a parity proof, while if no branch produces one then the 600-cell contains no parity proofs of the target size $R$-$B$. The search becomes slower with increasing values of $R$ and/or $B$, and also as the number of rays occurring four times in the target set increases, and so we were not able to carry out the search exhaustively for all values of $R$ and $B$. Additional calculations were done after the initial search to eliminate sets that corresponded to duplicate or non-critical proofs.

We now give a couple of examples of parity proofs. A first example is given in Table 4. It shows two 30-15 proofs that are complementary to each other in the sense that they have no rays in common. There are exactly 120 such pairs of complementary proofs, and a simple construction for them is given in the Appendix. Figure 1 shows an alternative representation of the two proofs in Table 4 by means of MMP hypergraphs [36]. The skeleton for each of the hypergraphs is a decagon whose alternate sides are bases from a single column of Table 4. The skeleton is then completed by five loops crisscrossing the figure that pick out the bases in the remaining column of Table 4.

A second example of a parity proof is given in Table 5. This table shows a 40-30 set containing a 34-17 and a 26-13 parity proof within it. MMP hypergraph representations of these proofs are shown in Fig. 2. The 34-17 proof has a decagonal loop of bases for its skeleton and the 26-13 proof an octagonal loop, with the remaining bases in both cases straddling different parts of the skeleton. Constructions for the parity proofs in Tables 4 and 5 based on the geometry of the 600-cell are given in the

**Table 4** Two complementary 30-15 parity proofs, one in plain type and the other in bold

| | A | B | C | D | E |
|---|---|---|---|---|---|
| A′ | 1 2 3 4<br>**9 10 11 12** | | **22 60 39 28**<br>18 47 33 55 | **57 23 27 40**<br>36 53 20 46 | |
| B′ | 13 14 15 16<br>**21 22 23 24** | | **34 12 51 40**<br>30 59 45 7 | **9 35 39 52**<br>48 5 32 58 | |
| C′ | **25 26 27 28**<br>29 30 31 32 | | **42 11 57 19**<br>37 56 14 5 | **60 17 44 10**<br>7 13 54 38 | |
| D′ | **41 42 43 44**<br>45 46 47 48 | | 58 36 15 4<br>**49 8 26 17** | 33 59 3 16<br>**19 25 6 50** | |
| E′ | **49 50 51 52**<br>53 54 55 56 | | **6 35 21 43**<br>1 20 38 29 | **24 41 8 34**<br>31 37 18 2 | |

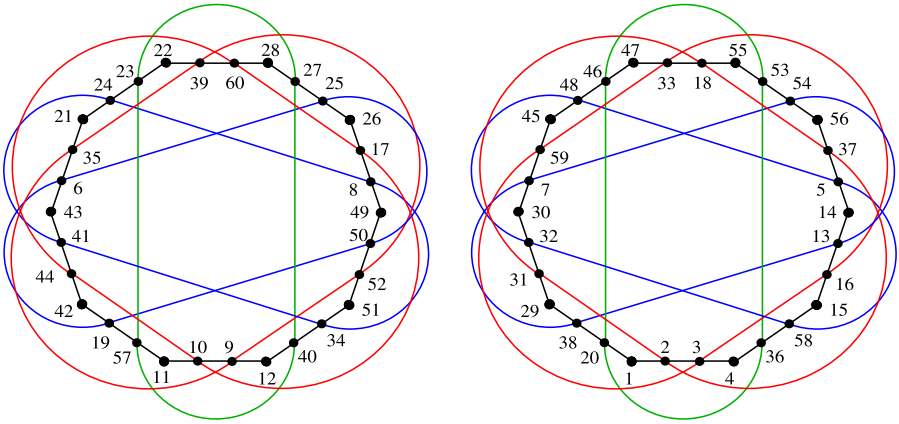


**Fig. 1** MMP hypergraphs [36] for the two 30-15 proofs shown in Table 4. The one on the *left* corresponds to the bold bases in Table 4 and the one on the *right* to the bases in regular type. Although these two hypergraphs have the same structure, the 30-15 sets they describe are geometrically distinct for the reason discussed in Sect. 4(ii)

Appendix. Several other examples of parity proofs, together with their constructions, can also be found there.

## 4 Discussion

We have pointed out the existence of a large number of $R$-$B$ (i.e., Ray-Basis) sets within the 600-cell that provide parity proofs of the BKS theorem. Some general observations can be made about these sets:

**Table 5** All 30 bases shown are those of a 40-30 set, and all the bold bases (*plain bold*, *bold italic* and *bold underlined*) are those of a 34-19 set. The two parity proofs are provided by a 34-17 set (whose bases are the *plain bold* and *bold underlined* ones) and a 26-13 set (whose bases are the *plain bold* and *bold italic* ones)

| | A | B | C | D | E |
|---|---|---|---|---|---|
| A′ | **5 6 7 8**<br>**9 10 11 12** | 38 24 58 25 | **22 60 39 28** | **57 23 27 40** | 59 26 37 21 |
| B′ | 17 18 19 20<br>**21 22 23 24** | **50 36 10 37** | ***34 12 51 40*** | ***9 35 39 52*** | **11 38 49 33** |
| C′ | 25 26 27 28<br>**33 34 35 36** | **20 9 41 59** | 42 11 57 19 | 60 17 44 10 | **58 43 12 18** |
| D′ | **37 38 39 40**<br>41 42 43 44 | **7 18 27 52** | 49 8 26 17 | 19 25 6 50 | **20 5 51 28** |
| E′ | **49 50 51 52**<br>**57 58 59 60** | 44 33 5 23 | **6 35 21 43** | **24 41 8 34** | 22 7 36 42 |

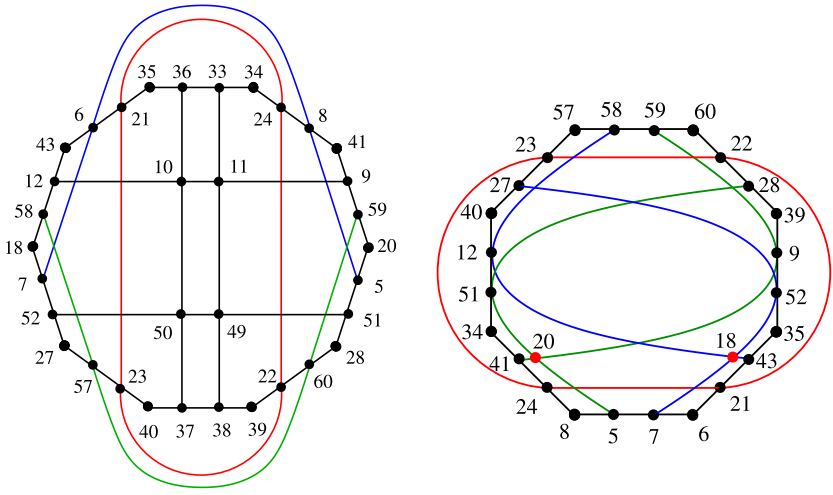


**Fig. 2** MMP hypergraphs for the 34-17 (*left*) and 26-13 (*right*) proofs shown in Table 5

(i) All the sets listed in Table 3 are basis-critical (as defined in Sect. 2). We checked this by means of a computer program.

(ii) Although Table 3 lists only 90 critical sets, the actual number is much larger, for two reasons. The first reason is that many of the sets in Table 3 come in a number of distinct varieties that are not equivalent to each other under the symmetries of the 600-cell. One example of this is provided by the 30-15 sets, of which

there are six different varieties. In addition to the two different varieties shown in Table 4 (which are really different, despite their structurally identical MMP diagrams), a third type is shown in Table 6 and there are three further types that we have not exhibited here. The differences between these types can be brought out by calculating the inner products of vectors in each of them, whereupon it will be found that the patterns of the inner products are not the same. These differences are experimentally significant, because the unitary transformations needed to transform the standard basis into the bases of each of these types are different. A few sets, such as the 26-13 set, come in only one variety, but the vast majority come in a number of different varieties. The second reason is that each of the geometrically distinct critical sets for a particular set of $R$ and $B$ values has many replicas (typically in the thousands) under the symmetries of the 600-cell. The combined effect of both these factors is to increase the total number of distinct parity proofs to somewhere in the vicinity of a hundred million.

(iii) We have limited our discussion in this paper only to critical sets that provide parity proofs of the BKS theorem. However the 600-cell has a large number of critical sets that provide non-parity proofs of the theorem. These proofs are not as transparent as the parity proofs, but they are just as conclusive. We explored them in part in Ref. [4] and will analyze and generate them extensively in Ref. [5].

(iv) The parity proofs of this paper can be used to devise experimental tests of noncontextuality of the sort proposed by Cabello [22, 23]. We recall how such a test works. For a $R$-$B$ set yielding a parity proof, let $A^i_j = 2|\psi^i_j\rangle\langle\psi^i_j| - 1$ ($i = 1, \ldots, B$, $j = 1, \ldots, 4$), where $|\psi^i_j\rangle$ is the normalized column vector corresponding to the $j$-th ray of the $i$-th basis (note that two or more of the $\psi^i_j$ with different values of $i$ and/or $j$ can be identical because the same ray generally occurs in several different bases). Each observable $A^i_j$ has only the eigenvalues $+1$ or $-1$. Cabello's argument implies that any noncontextual hidden variables theory (NHVT) obeys the inequality

$$\sum_{i=1}^{B} -\langle A^i_1 A^i_2 A^i_3 A^i_4\rangle \leq M, \tag{1}$$

where the averages $\langle\rangle$ above are to be taken over an ensemble of runs and $M$ is an upper bound. Quantum mechanics predicts that (1) holds as an equality with $M = B$, but NHVTs predict (see next paragraph) that the above inequality holds with $M$ equal to $B - 2$ at most. This is the contradiction between a NHVT and quantum mechanics that can be put to experimental test.

We now give the argument leading to the maximum value of $M$, namely, $B - 2$. According to a NHVT, each observable $A^i_j$ has the definite value of $+1$ or $-1$ in any quantum state, independent of the other observables with which it is measured. Consider the expression on the left side of (1), but without the averaging $\langle\rangle$ over many runs, and denote it by $F$. The maximum value of $F$ in any run is $B$, and it is achieved when each term in it has the value of $+1$. Let us see how the values of the various $A^i_j$ can be chosen so that this maximum is

achieved. Clearly, one or three of the $A^i_j$'s in each term of $F$ must be equal to $-1$ for this to happen. Let the number of terms with one $A^i_j$ equal to $-1$ be $n$ and the number with three $A^i_j$'s equal to $-1$ be $m$. Then, if we choose the values of the $A^i_j$'s in such a way that $n + m = B$, we can guarantee that $F = B$. But an obstacle looms that prevents us from reaching this goal. The total number of $-1$'s occurring over all the bases is $n + 3m = B + 2m$ (since $n + m = B$). The difficulty now is that $B + 2m$ is required to be both odd and even (odd because $B$ is odd, and even because the number of $-1$'s in all the bases is required to be even for the parity proof to be valid). This contradiction shows that a NHVT theory cannot make the value of $F$ equal to $B$. The best it can do is to make all but one of the terms in $F$ equal to $+1$, and this limits the maximum value of $F$ to $B - 2$. Averaging the value of $F$ over a large number of runs could make the quantity on the left side of (1) dip below the upper bound of $B - 2$, according to a NHVT.

For any basis-critical parity proof, quantum mechanics predicts that (1) holds as an equality with $M = B$ whereas a NHVT predicts that $M = B - 2$ (since value assignments can always be found that make $B - 1$ of the terms on the left of (1) equal to 1 and one term equal to $-1$). A 18-9 parity proof thus leads to the ratio of 7/9 for the bounds due to NHVTs and quantum mechanics. This bound can be improved slightly by considering all 1800 26-13 parity proofs within the 60-75 set. Of the 75 terms on the left side of (1), at least 9 must then contribute $-1$ to the sum, causing the previous ratio to dip to 57/75, which is very slightly less than 7/9. Whether a further improvement can be effected by simultaneous consideration of a larger number of parity proofs is an open question.

It is worth stressing that the contradiction we have demonstrated between NHVTs and quantum mechanics generalizes in a straightforward manner to any parity proof in any even dimension greater than or equal to 4. Parity proofs of the type we are considering are not possible in odd dimensions, so a similar conflict cannot be demonstrated in this case.

(v) Any parity proof of the BKS theorem (or even a non-parity proof) can be turned into a scheme for quantum key distribution, as pointed out in [33]. The idea is simple: since there are no hidden variables that model the observables in a BKS proof, there is no data in the transmitted particles to be stolen while the key is being established; the key comes into being only after sender and receiver exchange messages to determine the cases in which they used the same bases to encode and decode their particles. The preferred bases in such a scheme, when they exist, are a maximal set of mutually unbiased bases. A maximal set of five mutually unbiased bases does indeed exist in four dimensions, and has been proposed for use in key distribution schemes based on four-state systems [37]. However, any set of bases leading to a BKS proof, such as the ones in this paper, can also be used. They may not be as efficient as schemes based on mutually unbiased bases, but they may be advantageous in some situations and would therefore seem to be worth exploring further.

## Appendix A

The purpose of this Appendix is to show how special geometrical features of the 600-cell can be exploited to give simple rules for generating many of the parity proofs in Table 3. We first review some basic geometrical facts about the 600-cell and then show how they can be used to arrive at the rules. Readers wanting a more detailed account of the geometrical properties of the 600-cell can consult the classic monograph by Coxeter [38].

The 600-cell is a regular polytope with 120 vertices distributed symmetrically on the surface of a four-dimensional sphere. The vertices come in antipodal pairs, and the 60 rays are the unoriented directions passing through antipodal pairs of vertices. If the vertices are taken to lie on a sphere of radius 2 centered at the origin, then the coordinates of 60 of the vertices can be chosen as in Table 1 and the remaining vertices are the antipodes of these.

### A.1 Facets of the 600-cell

Any finite subset of rays of the 600-cell will be termed a **facet**. There are several facets that will play an important role in the constructions below. We now define these facets and depict them by their Kochen-Specker (KS) diagrams in Fig. 3. In a KS diagram, rays are represented by dots and dots corresponding to orthogonal pairs of rays are joined by lines.

The simplest type of facet is a single ray, which we will also term a **point**. Rays/points will be referred to by the numbers assigned to them in Table 1.

Four mutually orthogonal rays make up a **basis**. The KS diagram of a basis can be taken as four dots at the corners of a square, with all the edges and diagonals of the square drawn in. A basis will be denoted by four numbers separated by spaces, e.g., 7 18 27 52, just as in Table 2.

Any three rays will be said to form a **line** if the coordinates of one of them can be expressed as a linear combination of those of the other two. For example, the points 3, 8 and 10 form a line, which we will denote (3 8 10). Two lines are said to be the duals of each other if every point (ray) on one is orthogonal to every point on the other. The lines (3 8 10) and (16 17 24) are the duals of each other and will be termed a **dual**

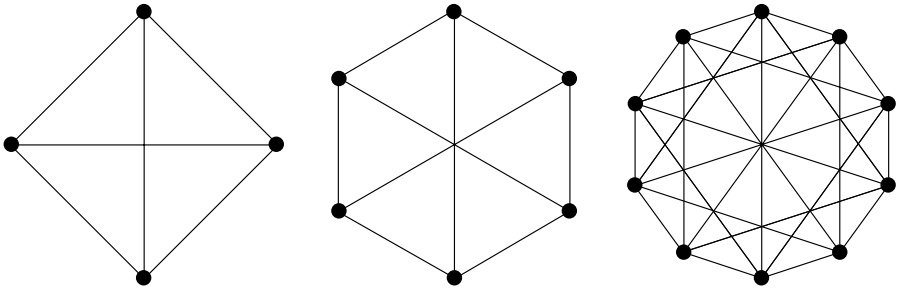

**Fig. 3** The Kochen-Specker diagrams of a basis (*left*), a dual line pair (DLP) (*center*) and a dual pentagon pair (DPP) (*right*)

**line pair** (DLP) and denoted (3 8 10) + (16 17 24). The KS diagram of a DLP takes on a simple form if the points of the dual lines are arranged at the alternate vertices of a hexagon; then the orthogonalities between the rays are represented by the six edges and three diameters of the hexagon. The geometry of the 600-cell is such that any set of six points having this KS diagram represents a dual line pair; the requirement that the points at the alternate vertices satisfy the conditions for a line need not be added because it turns out to be satisfied automatically.

A **pentagon** is any set of five rays with the property that five pairs among them have an absolute inner product of $\tau$ and the remaining five an absolute inner product of $\kappa$. The points 1, 15, 30, 47 and 56 form a pentagon, which we will denote (1 15 30 47 56). Two pentagons will be said to be the duals of one another if every point of one is orthogonal to every point of the other. The pentagons (1 15 30 47 56) and (4 14 29 45 55) are the duals of each other and will be said to be a **dual pentagon pair** (DPP). A symbol for a DPP will be introduced in the next subsection. If the points corresponding to a dual pair of pentagons are arranged at the alternate vertices of a decagon, then the KS diagram of the DPP takes on a very simple form: it consists of the ten edges and five diameters of the decagon, together with ten of its diagonals (see Fig. 3). Again, it turns out that any set of ten points possessing this KS diagram constitutes a DPP, with the conditions for the points at alternate vertices to form pentagons being automatically satisfied.

The most complex facet of interest to us is a **Reye's configuration** (RC), which is a set of 12 "points" and 16 "lines" with the property that three "points" lie on every "line" and four "lines" pass through every "point". If the terms "points" and "lines" in this definition are taken to be identical with the points and lines defined above, it is easy to check that points 1 through 12 form a RC with the 16 lines being given by (1 5 9), (1 6 10), (1 7 11), (1 8 12), (2 5 10), (2 6 9), (2 7 12), (2 8 11), (3 5 11), (3 6 12), (3 7 9), (3 8 10), (4 5 12), (4 6 11), (4 7 10) and (4 8 9). An equivalent definition of a RC is that it consists of the rays in three mutually unbiased bases (i.e. bases with the property that the magnitude of the inner product of any normalized ray of one with any normalized ray of the other is always the same). In the case of the 600-cell this latter definition guarantees that the 12 rays in the three bases form 16 lines, with one point of each line coming from each of the three bases. In the example of the RC just given, the three (mutually unbiased) bases are 1 2 3 4, 5 6 7 8 and 9 10 11 12.

The above discussion has been carried out in projective or ray space. However, many of the facets correspond to familiar figures in four-dimensional Euclidean space if one recalls that each point in projective space corresponds to a pair of mutually inverse points in Euclidean space. Then a basis corresponds to a **16-cell** (or **cross polytope**), a pair of mutually unbiased bases to a **8-cell** (or **hypercube**), and three mutually unbiased bases (or a RC) to a **24-cell**. These three figures are all convex regular polytopes in four dimensions (just like the 600-cell), and their bounding cells consist of 16 tetrahedra, 8 cubes and 24 octahedra, respectively.

### A.2 Tilings of the 600-cell by Its Facets

A particular type of facet (e.g. bases) will be said to tile the 600-cell if the union of several mutually disjoint specimens of that type yields all 60 rays of the 600-cell. The

600-cell has many tilings by its bases, DLPs, DPPs and RCs. We now discuss these tilings one by one.

First consider the bases. The 600-cell has 75 bases in it, which are shown in Table 2. The three bases in any block make up a RC, and the $5 \times 5$ array of blocks shows the 25 different RCs in the 600-cell. The five RCs in any row or column of the array give a tiling of the 600-cell. There are exactly ten such tilings, one associated with each row or column of the array. These tilings were first discovered by the Dutch geometer P.H. Schoute [38], who observed that the 600-cell has five mutually disjoint 24-cells inscribed in it in ten different ways. The letters in Table 2 help in reconstructing these tilings from the 24-cells: if each RC (or 24-cell) is labeled by a pair of letters, a primed one and an unprimed one, then arranging the RCs so that all the RCs in a row (or column) share a primed (or unprimed) letter reproduces the tilings. The tilings by bases are a trivial consequence of the tilings by RCs: each of the latter gives rise to a tiling by 15 bases.

Next consider the DLPs. The 600-cell has 100 DLPs in it and they are arranged in a $10 \times 10$ array in Table 10. The ten DLPs in any row or column of this array give a tiling of the 600-cell, there being 20 such tilings in all. Finally consider the DPPs. There are 36 DPPs in the 600-cell and they are arranged in a $6 \times 6$ array in Table 11. The six DPPs in any row or column of this array give a tiling of the 600-cell, there being 12 such tilings in all. For later reference we will label the DPPs in Table 11 from 1 to 36, proceeding from left to right and top to bottom. Thus, the DPP in the third row and second column will be referred to as DPP14 and the one in the last row and fifth column as DPP35.

The basis table, DLP table and DPP table are closely related in several ways. As one example of this, we show how the basis table can be reconstructed from any row or column of the DPP table. Any two DPPs from the same row or column of Table 11 can be "mated" to produce five bases, with half the rays of each basis coming from each of the DPPs. Since there are 15 pairings of the DPPs in a row or column, each of which gives rise to five bases, the total number of bases that can be produced in this way is 75, which are all the bases of the 600-cell. The rows and columns of the DPP table allow the basis table to be recovered in 12 different ways.

### A.3 Deletion of Rays; Isogonal Subsets of the 60-ray System

By deletion of a set of rays from a $R$-$B$ set, we will mean dropping all bases involving any of these rays from this set to obtain a new set, $R'$-$B'$, with $R' < R$ and $B' < B$. Deletion of rays is a crucial step in the construction of all the critical sets to be presented below.

The 600-cell, as well as the 60-75 system of rays and bases derived from it, is isogonal (or vertex/ray-transitive) in the sense that there are symmetry operations that take any vertex (or ray) into any other vertex (or ray) while keeping the structure as a whole invariant. It turns out that the 60-75 set has a number of isogonal subsets within it, which may be obtained by deleting any number of DPPs (from one to five) from an arbitrary row or column of Table 11. Deletion of one, two or three DPPs from any row or column of Table 11 from the 60-75 set reduces it to a 50-50, 40-30 or 30-15 set, respectively. The basis tables of these sets are decimated versions of

Table 2, with 25, 35 or 45 bases dropped, respectively. The number of different 50-50, 40-30 and 30-15 sets is 36, 180 and 240, respectively. These smaller isogonal sets are interesting because they each contain a large number of critical sets and can be searched far more easily for these sets than the full 60-75 set. We will ignore the sets obtained by deleting four or more DPPs from a row or column of Table 11 because they do not contain any critical sets.

### A.4 Constructions for some Critical Sets

We now use the ideas and tools developed in the previous subsections to give constructions for some of the parity proofs in Table 3.

#### *A.4.1 30-15 Set (Type-1)*

A somewhat involved construction for this set was given in [1], based on the deletion of DLPs. However a much simpler procedure is to delete any three DPPs from the same row or column of Table 11 from the 60-75 set. It was pointed out in Sect. A.3 that this procedure gives rise to 240 isogonal 30-15 sets. Inspection of these sets shows that they all provide parity proofs of the BKS theorem! An interesting feature of these sets is that they come in 120 complementary pairs, with the members of each pair having no rays in common. The two members of a pair are obtained by deleting distinct triads of DPPs from the same row or column of Table 11. For example, for the complementary pairs shown in Table 4, the one in bold is obtained by deleting DPPs 1, 2 and 3 and the one in plain type by deleting DPPs 4, 5 and 6. Alternatively, the former set is obtained by keeping all bases involving only the rays in DPPs 4, 5 and 6 and the latter by keeping all bases involving only the rays in DPPs 1, 2 and 3. These sets have been termed Type-1 because they are geometrically distinct from the Type-2 30-15 sets to be presented a little later.

The MMP hypergraphs of Fig. 1 have a nice interpretation in terms of DPPs. The points at the vertices of each decagon represent a DPP, with alternate vertices representing its two component pentagons. The two points within each edge in an alternating set of edges of the decagon also represent a DPP, there being two such DPPs. For each of the latter DPPs, the two points on an edge come from dual pentagons, and again the points alternate between the pentagons as one goes around the loop. It was pointed out in Sect. A.2 that any two DPPs mate to produce five bases, with two rays in each of the bases coming from each of the DPPs. This explains how the 15 bases arise in each of the hypergraphs: the bases corresponding to the edges arise from the matings between the distinguished DPP (corresponding to the decagon vertices) and each of the others, while the bases that straddle the figure arise from the matings of the other two DPPs with each other.

#### *A.4.2 34-17 Set*

This set can be constructed as follows:

(i) Pick a 40-30 set by deleting any two DPPs from the same row or column of Table 11. For example, deleting DPPs 1 and 2 gives the 40-30 set shown in Table 5.

(ii) Delete any DLP from this 40-30 set to get a 34-19 set. For example, deleting the DLP (5 24 57) + (8 23 58) leads to the 34-19 set in Table 5 whose bases are shown in plain boldface, italic boldface and underlined boldface.

(iii) The 34-19 set has 8 rays that each occur thrice in it and 26 rays that each occur twice. The 8 rays that each occur thrice form two bases made up of just themselves; these are the italic boldface bases in Table 5. Dropping these bases from the 34-19 set gives a 34-17 set.

The number of 34-17 sets that can be constructed in this way is the product of the number of 40-30 sets that can be picked in step (i) (= 180) and the number of DLPs that can be deleted in step (ii) (= 20), or 3600.

*A.4.3 26-13 Set*

A 26-13 set can be constructed by modifying the above procedure slightly. One keeps steps (i) and (ii), but replaces (iii) by the following alternative step:

(iii′) Write the two italic boldface bases in Table 5 (that were dropped in getting the 34-17 set) horizontally, one below the other, in such a way that each vertical pair of rays can be augmented by two additional rays to form a basis. This is done below, with the eight added rays indicated in boldface. The eight added rays (which are always unique) lead to six new bases, four along the columns of the array and two more along its last two rows. These six new bases are all present in Table 5 and are the underlined boldfaced ones. Dropping these bases from the 34-19 set gives a 26-13 set.

| | | | |
|---|---|---|---|
| 9 | 35 | 39 | 52 |
| 12 | 34 | 40 | 51 |
| **10** | **36** | **37** | **50** |
| **11** | **33** | **38** | **49** |

It might appear that the number of 26-13 sets that can be constructed in this way is the same as the number of 34-17 sets, or 3600. However it turns out that every 26-13 set is obtained twice by this method, so that their true number is 1800. As an illustration of this, the 26-13 set in Table 5 can also be constructed by first deleting DPPs 21 and 24, then deleting the DLP (3 19 56) + (4 17 54) and finally truncating the resulting 34-19 set in the manner described in step (iii′).

*A.4.4 38-19 Set*

The procedure for constructing this set is as follows:

(i) Choose a 50-50 set by deleting an arbitrary DPP. For example, deleting DPP1 leads to the 50-50 set shown in Table 6.

(ii) This 50-50 set (like all 50-50 sets) has 50 DLPs in it. Define the separation of two DLPs as the number of orthogonalities of rays between the two. It turns out that any 50-50 set has exactly 100 pairs of DLPs of separation 12. Deleting any such pair from a 50-50 set will lead to a 38-21 set. In the example of Table 6, deleting the DLPs (5 19 46) + (6 20 48) and (7 34 53) + (8 36 54) leads to the 38-21 set whose bases are the ones shown in plain boldface, italic boldface and underlined boldface.

**Table 6** All 50 bases are those of a 50-50 set and all the bold bases (*plain bold*, ***bold italic*** and ***bold underlined***) are those of a 38-21 set. The two parity proofs are provided by a 38-19 set (whose bases are the *plain bold* and ***bold underlined*** ones) and a 30-15 set (whose bases are the *plain bold* and ***bold italic*** ones)

| | A | | | | B | | | | C | | | | D | | | | E | | | |
|---|---|---|---|---|---|---|---|---|---|---|---|---|---|---|---|---|---|---|---|---|
| | | | | | **31** | **42** | **51** | **16** | **22** | **60** | **39** | **28** | **57** | **23** | **27** | **40** | | | | |
| A′ | 5 | 6 | 7 | 8 | **38** | **24** | **58** | **25** | | | | | 36 | 53 | 20 | 46 | **59** | **26** | **37** | **21** |
| | **9** | **10** | **11** | **12** | | | | | **13** | **32** | **50** | **41** | | | | | 34 | 19 | 48 | 54 |
| | | | | | 43 | 54 | 3 | 28 | 34 | 12 | 51 | 40 | **9** | **35** | **39** | **52** | | | | |
| B′ | 17 | 18 | 19 | 20 | 50 | 36 | 10 | 37 | | | | | 48 | 5 | 32 | 58 | **11** | **38** | **49** | **33** |
| | **21** | **22** | **23** | **24** | | | | | 25 | 44 | 2 | 53 | | | | | 46 | 31 | 60 | 6 |
| | **25** | **26** | **27** | **28** | | | | | 46 | 24 | 3 | 52 | | | | | 8 | 53 | 39 | 16 |
| C′ | | | | | 2 | 48 | 22 | 49 | 42 | 11 | 57 | 19 | **60** | **17** | **44** | **10** | | | | |
| | 33 | 34 | 35 | 36 | 20 | 9 | 41 | 59 | | | | | 7 | 13 | 54 | 38 | **58** | **43** | **12** | **18** |
| | ***37*** | ***38*** | ***39*** | ***40*** | 7 | 18 | 27 | 52 | | | | | **33** | **59** | **3** | **16** | 20 | 5 | 51 | 28 |
| D′ | **41** | **42** | **43** | **44** | | | | | 54 | 23 | 9 | 31 | | | | | **35** | **2** | **13** | **57** |
| | | | | | 32 | 21 | 53 | 11 | 49 | 8 | 26 | 17 | 19 | 25 | 6 | 50 | | | | |
| | **49** | **50** | **51** | **52** | | | | | 10 | 48 | 27 | 16 | | | | | **32** | **17** | **3** | **40** |
| E′ | | | | | 26 | 12 | 46 | 13 | 6 | 35 | 21 | 43 | 24 | 41 | 8 | 34 | | | | |
| | ***57*** | ***58*** | ***59*** | ***60*** | 44 | 33 | 5 | 23 | | | | | **31** | **37** | **18** | **2** | 22 | 7 | 36 | 42 |

(iii) The 38-21 set has 8 rays that each occur thrice in it and 30 rays that each occur twice. The 8 rays that each occur thrice form two bases made up of just themselves; these are the italic boldface bases in Table 6. Dropping these bases from the 38-21 set gives a 38-19 set.

The number of 38-19 sets that can be constructed by this method is the product of the number of 50-50 sets that can be picked in the first step (= 36) and the number of pairs of DLPs of separation 12 that can be deleted in the second step (= 100), or 3600.

### *A.4.5 30-15 Set (Type 2)*

This set can be obtained from a 38-21 set in a manner similar to that in which a 26-13 set is obtained from a 34-17 set. After carrying out steps (i) and (ii) for the 38-19 set just discussed, replace step (iii) by the following alternative step:

(iii′) Write the two italic boldface bases in Table 6 (that were dropped in getting the 38-19 set) horizontally, one below the other, in such a way that each vertical pair of rays can be augmented by two additional rays to form a basis. This is shown below, with the eight added rays indicated in boldface.

| | | | |
|---|---|---|---|
| 37 | 38 | 39 | 40 |
| 59 | 58 | 60 | 57 |
| **21** | **24** | **22** | **23** |
| **26** | **25** | **28** | **27** |

**Table 7** Two 50-25 parity proofs, one in *plain* type and the other in ***boldface***, both involving the same 50 rays but having no bases in common

| | A | | | | B | | | | C | | | | D | | | | E | | | |
|---|---|---|---|---|---|---|---|---|---|---|---|---|---|---|---|---|---|---|---|---|
| | **1** | **2** | **3** | **4** | **31** | **42** | **51** | **16** | | | | | | | | | **44** | **29** | **15** | **52** |
| A′ | | | | | **38** | **24** | **58** | **25** | **18** | **47** | **33** | **55** | **36** | **53** | **20** | **46** | **59** | **26** | **37** | **21** |
| | **9** | **10** | **11** | **12** | | | | | **13** | **32** | **50** | **41** | **43** | **49** | **30** | **14** | | | | |
| | 13 | 14 | 15 | 16 | | | | | **34** | **12** | **51** | **40** | **9** | **35** | **39** | **52** | | | | |
| B′ | **17** | **18** | **19** | **20** | 50 | 36 | 10 | 37 | | | | | | | | | 11 | 38 | 49 | 33 |
| | | | | | **8** | **57** | **29** | **47** | 25 | 44 | 2 | 53 | 55 | 1 | 42 | 26 | **46** | **31** | **60** | **6** |
| | | | | | 55 | 6 | 15 | 40 | 46 | 24 | 3 | 52 | 21 | 47 | 51 | 4 | 8 | 53 | 39 | 16 |
| C′ | 29 | 30 | 31 | 32 | | | | | 42 | 11 | 57 | 19 | 60 | 17 | 44 | 10 | | | | |
| | 33 | 34 | 35 | 36 | 20 | 9 | 41 | 59 | | | | | | | | | 58 | 43 | 12 | 18 |
| | **37** | **38** | **39** | **40** | | | | | **58** | **36** | **15** | **4** | **33** | **59** | **3** | **16** | | | | |
| D′ | **41** | **42** | **43** | **44** | **14** | **60** | **34** | **1** | | | | | | | | | **35** | **2** | **13** | **57** |
| | | | | | **32** | **21** | **53** | **11** | **49** | **8** | **26** | **17** | **19** | **25** | **6** | **50** | **10** | **55** | **24** | **30** |
| | 49 | 50 | 51 | 52 | 19 | 30 | 39 | 4 | | | | | | | | | 32 | 17 | 3 | 40 |
| E′ | | | | | 26 | 12 | 46 | 13 | 6 | 35 | 21 | 43 | 24 | 41 | 8 | 34 | 47 | 14 | 25 | 9 |
| | 57 | 58 | 59 | 60 | | | | | 1 | 20 | 38 | 29 | 31 | 37 | 18 | 2 | | | | |

The eight added rays (which are unique) lead to six new bases, four along the columns of the array and two more along its last two rows. These six new bases are all present in Table 6 and are the underlined boldfaced ones. Dropping these bases from the 38-21 set gives a Type-2 30-15 set. The number of such sets is the same as the number of 38-21 sets, or 3600. Note that we have called this 30-15 set a Type-2 set to distinguish it from the one constructed in Appendix A.4.1 These two types of 30-15 sets are geometrically distinct in that the rays of one cannot be made to pass into those of the other by any rotation in four-dimensional space.

### *A.4.6 50-25 Set*

This set can be constructed by deleting an arbitrary DPP from the 60-75 set to obtain a 50-50 set and then dividing the latter (in 291 ways) into a pair of 50-25 sets. The two 50-25 sets that are obtained in this way involve the same 50 rays but have no bases in common. The sets shown in Table 7 were obtained by deleting DPP10 and then partitioning the bases.

The total number of 50-25 sets that can be constructed in this way is the product of the number of 50-50 sets that can be picked in the first step (= 36) and the number of 50-25 sets into which each can be divided (= 2 × 291), or 20,952.

### *A.4.7 54-27 Set*

The construction of this set is similar to the last, but with a small twist. This time one deletes an arbitrary DLP from the 60-75 set to get a 54-54 set and then divides the latter (in 368 ways) into two 54-27 sets. The sets shown in Table 8 were obtained by deleting the DLP (5,19,46)+(6,20,48) and then partitioning the bases. The number of

**Table 8** Two 54-27 parity proofs, one in *plain* type and the other in *boldface*, both involving the same 54 rays but having no bases in common

| | A | | | | B | | | | C | | | | D | | | | E | | | |
|---|---|---|---|---|---|---|---|---|---|---|---|---|---|---|---|---|---|---|---|---|
| | **1** | **2** | **3** | **4** | **31** | **42** | **51** | **16** | **22** | **60** | **39** | **28** | 57 | 23 | 27 | 40 | **44** | **29** | **15** | **52** |
| A′ | | | | | **38** | **24** | **58** | **25** | **18** | **47** | **33** | **55** | | | | | 59 | 26 | 37 | 21 |
| | **9** | **10** | **11** | **12** | **56** | **45** | **17** | **35** | **13** | **32** | **50** | **41** | **43** | **49** | **30** | **14** | | | | |
| | 13 | 14 | 15 | 16 | 43 | 54 | 3 | 28 | **34** | **12** | **51** | **40** | 9 | 35 | 39 | 52 | 56 | 41 | 27 | 4 |
| B′ | | | | | **50** | **36** | **10** | **37** | **30** | **59** | **45** | **7** | | | | | 11 | 38 | 49 | 33 |
| | **21** | **22** | **23** | **24** | **8** | **57** | **29** | **47** | 25 | 44 | 2 | 53 | 55 | 1 | 42 | 26 | | | | |
| | **25** | **26** | **27** | **28** | | | | | | | | | 21 | 47 | 51 | 4 | 8 | 53 | 39 | 16 |
| C′ | 29 | 30 | 31 | 32 | | | | | | | | | 60 | 17 | 44 | 10 | 23 | 50 | 1 | 45 |
| | 33 | 34 | 35 | 36 | | | | | | | | | 7 | 13 | 54 | 38 | 58 | 43 | 12 | 18 |
| | **37** | **38** | **39** | **40** | **7** | **18** | **27** | **52** | **58** | **36** | **15** | **4** | **33** | **59** | **3** | **16** | | | | |
| D′ | **41** | **42** | **43** | **44** | **14** | **60** | **34** | **1** | **54** | **23** | **9** | **31** | 12 | 29 | 56 | 22 | **35** | **2** | **13** | **57** |
| | | | | | **32** | **21** | **53** | **11** | **49** | **8** | **26** | **17** | | | | | 10 | 55 | 24 | 30 |
| | 49 | 50 | 51 | 52 | | | | | | | | | 45 | 11 | 15 | 28 | 32 | 17 | 3 | 40 |
| E′ | **53** | **54** | **55** | **56** | | | | | | | | | 24 | 41 | 8 | 34 | 47 | 14 | 25 | 9 |
| | 57 | 58 | 59 | 60 | | | | | | | | | 31 | 37 | 18 | 2 | 22 | 7 | 36 | 42 |

**Table 9** A 36-19 parity proof (bases in *plain* type and *bold*) and a 32-17 parity proof (bases in *plain* type and *bold italics*). Each proof has two rays that occur four times each (rays 25 and 29 in both cases), with all the remaining rays occurring twice each

| | A | | | | B | | | | C | | | | D | | | | E | | | |
|---|---|---|---|---|---|---|---|---|---|---|---|---|---|---|---|---|---|---|---|---|
| | 1 | 2 | 3 | 4 | | | | | | | | | | | | | 44 | 29 | 15 | 52 |
| A′ | | | | | 38 | 24 | 58 | 25 | | | | | **36** | **53** | **20** | **46** | | | | |
| | | | | | | | | | 13 | 32 | 50 | 41 | | | | | | | | |
| | 13 | 14 | 15 | 16 | | | | | | | | | **9** | **35** | **39** | **52** | | | | |
| B′ | | | | | | | | | | | | | | | | | | | | |
| | | | | | 8 | 57 | 29 | 47 | 25 | 44 | 2 | 53 | | | | | 46 | 31 | 60 | 6 |
| | | | | | | | | | ***46*** | ***24*** | ***3*** | ***52*** | | | | | ***8*** | ***53*** | ***39*** | ***16*** |
| C′ | 29 | 30 | 31 | 32 | | | | | | | | | | | | | | | | |
| | **33** | **34** | **35** | **36** | ***20*** | ***9*** | ***41*** | ***59*** | | | | | | | | | | | | |
| | | | | | | | | | | | | | **33** | **59** | **3** | **16** | | | | |
| D′ | | | | | | | | | | | | | | | | | | | | |
| | | | | | | | | | | | | | 19 | 25 | 6 | 50 | | | | |
| | | | | | 19 | 30 | 39 | 4 | | | | | | | | | | | | |
| E′ | | | | | | | | | | | | | **24** | **41** | **8** | **34** | 47 | 14 | 25 | 9 |
| | 57 | 58 | 59 | 60 | | | | | 1 | 20 | 38 | 29 | | | | | | | | |

54-27 sets that can be constructed in this way is the product of the number of 54-54 sets that can be picked in the first step (= 100) and the number of 54-27 sets into which each can be divided (= 2 × 368), or 73,600.

**Table 10** The 100 dual line pairs (DLPs) of the 600-cell. The DLPs in any *row* or *column* provide a tiling of the 600-cell. The letters at the beginning of *each row* and *column* help identify the pair of 24-cells in which each line of a DLP originates. For example, the line (1 5 9) originates in AA' and DB', while (14 20 23) originates in AB' and DA'

| | | *A* *B* | | *A* *C* | | *A* *D* | | *A* *E* | | *B* *C* | | *B* *D* | | *B* *E* | | *C* *D* | | *C* *E* | | *D* *E* | |
|---|---|---|---|---|---|---|---|---|---|---|---|---|---|---|---|---|---|---|---|---|---|
| A′ | B′ | 3 | 16 | 2 | 13 | 1 | 14 | 4 | 15 | 25 | 28 | 35 | 36 | 31 | 29 | 32 | 30 | 33 | 34 | 27 | 26 |
| | | 8 | 17 | 7 | 18 | 5 | 20 | 6 | 19 | 45 | 47 | 42 | 43 | 38 | 37 | 39 | 40 | 41 | 44 | 46 | 48 |
| | | 10 | 24 | 12 | 22 | 9 | 23 | 11 | 21 | 51 | 50 | 58 | 57 | 56 | 54 | 55 | 53 | 60 | 59 | 49 | 52 |
| A′ | C′ | 2 | 25 | 3 | 28 | 4 | 27 | 1 | 26 | 24 | 22 | 17 | 20 | 16 | 15 | 13 | 14 | 18 | 19 | 23 | 21 |
| | | 6 | 31 | 5 | 32 | 7 | 30 | 8 | 29 | 42 | 41 | 38 | 40 | 45 | 48 | 47 | 46 | 39 | 37 | 43 | 44 |
| | | 9 | 35 | 11 | 33 | 10 | 36 | 12 | 34 | 56 | 55 | 51 | 49 | 58 | 59 | 60 | 57 | 50 | 52 | 53 | 54 |
| A′ | D′ | 1 | 38 | 4 | 39 | 3 | 40 | 2 | 37 | 17 | 18 | 16 | 14 | 24 | 21 | 22 | 23 | 13 | 15 | 20 | 19 |
| | | 7 | 42 | 8 | 41 | 6 | 43 | 5 | 44 | 31 | 32 | 25 | 27 | 35 | 34 | 33 | 36 | 28 | 26 | 30 | 29 |
| | | 11 | 45 | 9 | 47 | 12 | 46 | 10 | 48 | 58 | 60 | 56 | 53 | 51 | 52 | 50 | 49 | 55 | 54 | 57 | 59 |
| A′ | E′ | 4 | 51 | 1 | 50 | 2 | 49 | 3 | 52 | 16 | 13 | 24 | 23 | 17 | 19 | 18 | 20 | 22 | 21 | 14 | 15 |
| | | 5 | 56 | 6 | 55 | 8 | 53 | 7 | 54 | 35 | 33 | 31 | 30 | 25 | 26 | 28 | 27 | 32 | 29 | 36 | 34 |
| | | 12 | 58 | 10 | 60 | 11 | 57 | 9 | 59 | 38 | 39 | 45 | 46 | 42 | 44 | 41 | 43 | 47 | 48 | 40 | 37 |
| B′ | C′ | 15 | 28 | 14 | 25 | 13 | 26 | 16 | 27 | 3 | 2 | 10 | 9 | 8 | 6 | 7 | 5 | 12 | 11 | 1 | 4 |
| | | 20 | 29 | 19 | 30 | 17 | 32 | 18 | 31 | 37 | 40 | 47 | 48 | 43 | 41 | 44 | 42 | 45 | 46 | 39 | 38 |
| | | 22 | 36 | 24 | 34 | 21 | 35 | 23 | 33 | 57 | 59 | 54 | 55 | 50 | 49 | 51 | 52 | 53 | 56 | 58 | 60 |
| B′ | D′ | 14 | 37 | 15 | 40 | 16 | 39 | 13 | 38 | 8 | 7 | 3 | 1 | 10 | 11 | 12 | 9 | 2 | 4 | 5 | 6 |
| | | 18 | 43 | 17 | 44 | 19 | 42 | 20 | 41 | 36 | 34 | 29 | 32 | 28 | 27 | 25 | 26 | 30 | 31 | 35 | 33 |
| | | 21 | 47 | 23 | 45 | 22 | 48 | 24 | 46 | 54 | 53 | 50 | 52 | 57 | 60 | 59 | 58 | 51 | 49 | 55 | 56 |
| B′ | E′ | 13 | 50 | 16 | 51 | 15 | 52 | 14 | 49 | 10 | 12 | 8 | 5 | 3 | 4 | 2 | 1 | 7 | 6 | 9 | 11 |
| | | 19 | 54 | 20 | 53 | 18 | 55 | 17 | 56 | 29 | 30 | 28 | 26 | 36 | 33 | 34 | 35 | 25 | 27 | 32 | 31 |
| | | 23 | 57 | 21 | 59 | 24 | 58 | 22 | 60 | 43 | 44 | 37 | 39 | 47 | 46 | 45 | 48 | 40 | 38 | 42 | 41 |
| C′ | D′ | 27 | 40 | 26 | 37 | 25 | 38 | 28 | 39 | 9 | 11 | 6 | 7 | 2 | 1 | 3 | 4 | 5 | 8 | 10 | 12 |
| | | 32 | 41 | 31 | 42 | 29 | 44 | 30 | 43 | 15 | 14 | 22 | 21 | 20 | 18 | 19 | 17 | 24 | 23 | 13 | 16 |
| | | 34 | 48 | 36 | 46 | 33 | 47 | 35 | 45 | 49 | 52 | 59 | 60 | 55 | 53 | 56 | 54 | 57 | 58 | 51 | 50 |
| C′ | E′ | 26 | 49 | 27 | 52 | 28 | 51 | 25 | 50 | 6 | 5 | 2 | 4 | 9 | 12 | 11 | 10 | 3 | 1 | 7 | 8 |
| | | 30 | 55 | 29 | 56 | 31 | 54 | 32 | 53 | 20 | 19 | 15 | 13 | 22 | 23 | 24 | 21 | 14 | 16 | 17 | 18 |
| | | 33 | 59 | 35 | 57 | 34 | 60 | 36 | 58 | 48 | 46 | 41 | 44 | 40 | 39 | 37 | 38 | 42 | 43 | 47 | 45 |
| D′ | E′ | 39 | 52 | 38 | 49 | 37 | 50 | 40 | 51 | 1 | 4 | 11 | 12 | 7 | 5 | 8 | 6 | 9 | 10 | 3 | 2 |
| | | 44 | 53 | 43 | 54 | 41 | 56 | 42 | 55 | 21 | 23 | 18 | 19 | 14 | 13 | 15 | 16 | 17 | 20 | 22 | 24 |
| | | 46 | 60 | 48 | 58 | 45 | 59 | 47 | 57 | 27 | 26 | 34 | 33 | 32 | 30 | 31 | 29 | 36 | 35 | 25 | 28 |

### *A.4.8 36-19 and 32-17 Sets*

In all the above proofs, each ray occurred twice among the bases. Table 9 shows two parity proofs, a 36-19 proof and a 32-17 proof, that both involve two rays occurring four times each.

**Table 11** The 36 Dual-Pentagon-Pairs (DPPs) of the 600-Cell. The DPPs in any *row* or *column* provide a tiling of the 600-cell

| | | | | | | | | | | | |
|---|---|---|---|---|---|---|---|---|---|---|---|
| 1 | 4 | 2 | 3 | 5 | 7 | 6 | 8 | 9 | 10 | 11 | 12 |
| 15 | 14 | 16 | 13 | 18 | 20 | 17 | 19 | 24 | 23 | 22 | 21 |
| 56 | 55 | 54 | 53 | 59 | 58 | 57 | 60 | 50 | 52 | 51 | 49 |
| 47 | 45 | 46 | 48 | 38 | 37 | 39 | 40 | 44 | 41 | 43 | 42 |
| 30 | 29 | 32 | 31 | 36 | 33 | 34 | 35 | 27 | 25 | 26 | 28 |
| 2 | 3 | 1 | 4 | 6 | 8 | 5 | 7 | 11 | 12 | 9 | 10 |
| 43 | 44 | 41 | 42 | 47 | 46 | 45 | 48 | 40 | 38 | 37 | 39 |
| 33 | 35 | 36 | 34 | 26 | 25 | 27 | 28 | 29 | 32 | 30 | 31 |
| 17 | 18 | 19 | 20 | 24 | 21 | 22 | 23 | 13 | 15 | 16 | 14 |
| 52 | 49 | 51 | 50 | 53 | 55 | 54 | 56 | 58 | 57 | 60 | 59 |
| 5 | 6 | 7 | 8 | 9 | 12 | 10 | 11 | 1 | 3 | 2 | 4 |
| 21 | 23 | 24 | 22 | 13 | 14 | 15 | 16 | 17 | 20 | 19 | 18 |
| 31 | 32 | 29 | 30 | 34 | 35 | 33 | 36 | 28 | 26 | 27 | 25 |
| 50 | 51 | 49 | 52 | 56 | 54 | 53 | 55 | 59 | 60 | 58 | 57 |
| 40 | 37 | 39 | 38 | 43 | 41 | 42 | 44 | 46 | 45 | 47 | 48 |
| 7 | 8 | 5 | 6 | 10 | 11 | 9 | 12 | 2 | 4 | 1 | 3 |
| 26 | 27 | 25 | 28 | 32 | 30 | 29 | 31 | 36 | 35 | 33 | 34 |
| 16 | 13 | 15 | 14 | 19 | 17 | 18 | 20 | 21 | 22 | 24 | 23 |
| 41 | 42 | 43 | 44 | 45 | 48 | 46 | 47 | 39 | 37 | 40 | 38 |
| 57 | 59 | 60 | 58 | 49 | 50 | 51 | 52 | 56 | 53 | 54 | 55 |
| 9 | 11 | 10 | 12 | 1 | 2 | 3 | 4 | 5 | 8 | 6 | 7 |
| 19 | 20 | 18 | 17 | 22 | 23 | 21 | 24 | 16 | 14 | 13 | 15 |
| 38 | 39 | 40 | 37 | 44 | 42 | 41 | 43 | 47 | 48 | 45 | 46 |
| 28 | 25 | 26 | 27 | 31 | 29 | 30 | 32 | 34 | 33 | 36 | 35 |
| 53 | 54 | 56 | 55 | 57 | 60 | 58 | 59 | 49 | 51 | 52 | 50 |
| 10 | 12 | 9 | 11 | 3 | 4 | 1 | 2 | 6 | 7 | 5 | 8 |
| 34 | 36 | 33 | 35 | 27 | 28 | 25 | 26 | 30 | 31 | 29 | 32 |
| 58 | 60 | 57 | 59 | 51 | 52 | 49 | 50 | 54 | 55 | 53 | 56 |
| 22 | 24 | 21 | 23 | 15 | 16 | 13 | 14 | 18 | 19 | 17 | 20 |
| 46 | 48 | 45 | 47 | 39 | 40 | 37 | 38 | 42 | 43 | 41 | 44 |

### *A.4.9 Basis-Complementary Parity Proofs*

The proofs in Tables 7 and 8 are particular instances of a phenomenon we term "basis complementarity", which is of interest because it forges a link between many pairs of proofs in Table 3 that might otherwise appear to be unrelated. Any $R$-$B$ set, with $B$ even, in which each ray occurs four times can potentially house many basis-complementary parity proofs within it. The 50-50 sets obtained by a deleting a DPP and the 54-54 sets obtained by deleting a DLP are both examples of such sets. If there is a $R$-$B$ parity proof contained in either of these sets, the remaining $N - B$ bases, which involve $N - 2B + R$ distinct rays (with $N = 50$ or 54), automatically yield another parity proof that we will term the "basis-complementary" proof to the original one. The basis-complementary proof has $2R - 2B$ rays that occur twice each and

$N - R$ rays that occur four times each. In general the proof complementary to a given proof might not be basis-critical, in which case it would be left out of Table 3. Only if both members of a basis-complementary pair are basis-critical would they both be included in Table 3. Three examples of basis-complementary (and basis-critical) parity proofs within a 50-50 set are 36-19/48-31, 39-21/47-29, and 42-21/50-29 and three examples within a 54-54 set are 37-19/53-35, 41-21/53-33 and 44-23/52-31. We hope to make several examples of such proofs available on the interactive website (see footnote 1).

**Acknowledgements** One of us (M. P.) would like to thank his host Hossein Sadeghpour at ITAMP. M. P.'s stay at ITAMP was Supported by the US National Science Foundation through a grant for the Institute for Theoretical Atomic, Molecular, and Optical Physics (ITAMP) at Harvard University and Smithsonian Astrophysical Observatory and Ministry of Science, Education, and Sport of Croatia through the project No. 082-0982562-3160. M. P. carried out his part of the computation on the cluster Isabella of the University Computing Centre of the University of Zagreb and on the Croatian National Grid Infrastructure.

## References

1. Waegell, M., Aravind, P.K.: J. Phys. A **43**, 105304 (2010)
2. Bell, J.S.: Rev. Mod. Phys. **38**, 447 (1966). Reprinted in J.S. Bell, Speakable and Unspeakable in Quantum Mechanics. Cambridge University Press, Cambridge (1987)
3. Kochen, S., Specker, E.P.: J. Math. Mech. **17**, 59 (1967)
4. Pavičić, M., Megill, N.D., Aravind, P.K.: arXiv:1004.1433 (2010)
5. Pavičić, M., Megill, N.D., Aravind, P.K., Waegell, M.: Unpublished (2010)
6. Peres, A.: J. Phys. A **24**, L175 (1991)
7. Kochen, S., Conway, J.H.: Quantum Theory: Concepts and Methods. Kluwer Academic, Dordrecht (1993). As quoted in A. Peres
8. Bub, J.: Found. Phys. **26**, 787 (1996)
9. Bub, J.: Interpreting the Quantum World. Cambridge University Press, Cambridge (1997), Chap. 3
10. Penrose, R.: In: Ellis, J., Amati, D. (eds.) Quantum Reflections, pp. 1–27. Cambridge University Press, Cambridge (2000)
11. Cabello, A., Estebaranz, J.M., García-Alcaine, G.: Phys. Lett. A **212**, 183 (1996)
12. Kernaghan, M.: J. Phys. A **27**, L829 (1994)
13. Zimba, J., Penrose, R.: Stud. Hist. Philos. Sci. **24**, 697 (1993)
14. Penrose, R.: Shadows of the Mind. Oxford University Press, Oxford (1994), Chap. 5
15. Pavičić, M., Merlet, J.P., McKay, B.D., Megill, N.D.: J. Phys. A **38**, 1577 (2005)
16. Pavičić, M., Merlet, J.P., Megill, N.D.: The French National Institute for Research in Computer Science and Control Research Reports RR-5388 (2004)
17. Pavičić, M., Megill, N.D., Merlet, J.P.: Phys. Lett. A **374**, 2122 (2010)
18. Kernaghan, M., Peres, A.: Phys. Lett. A **198**, 1 (1995)
19. Conway, J.H., Kochen, S.B.: In: Bertlmann, R.A., Zeilinger, A. (eds.) Quantum [Un]speakables: From Bell to Quantum Information, pp. 257–269. Springer, Berlin (2002)
20. DiVincenzo, D., Peres, A.: Phys. Rev. A **55**, 4089 (1997)
21. Ruuge, A.E., Van Oystaeyen, F.: J. Math. Phys. **46**, 052109 (2005)
22. Cabello, A.: Phys. Rev. Lett. **101**, 210401 (2008)
23. Badziag, P., Bengtsson, I., Cabello, A., Pitowsky, I.: Phys. Rev. Lett. **103**, 050401 (2009)
24. Kirchmair, G., Zähringer, F., Gerritsma, R., Kleinmann, M., Gühne, O., Cabello, A., Blatt, R., Roos, C.F.: Nature **460**, 494 (2009)
25. Bartosik, H., Klep, J., Schmitzer, C., Sponar, S., Cabello, A., Rauch, H., Hasegawa, Y.: Phys. Rev. Lett. **103**, 040403 (2009)
26. Amselem, E., Rådmark, M., Bourennane, M., Cabello, A.: Phys. Rev. Lett. **103**, 160405 (2009)
27. Moussa, O., Ryan, C.A., Cory, D.G., Laflamme, R.: Phys. Rev. Lett. **104**, 160501 (2010)
28. Klyashko, A.A., Can, M.A., Binicioglu, S., Shumovsky, A.S.: Phys. Rev. Lett. **101**, 020403 (2008)
29. Cabello, A.: Phys. Rev. A **82**, 032110 (2010)

30. Cabello, A., Severini, S., Winter, A.: arXiv:1010.2163v1 (2010)
31. Cabello, A.: Phys. Rev. Lett. **104**, 2210401 (2010)
32. Liang, Y.C., Spekkens, R.W., Wiseman, H.M.: arXiv:1010.1273v1 (2010)
33. Bechmann-Pasquinucci, H., Peres, A.: Phys. Rev. Lett. **85**, 3313 (2000)
34. Svozil, K.: Phys. Rev. A **79**, 054306 (2009)
35. Spekkens, R.W., Buzacott, D.H., Keehn, A.J., Toner, B., Pryde, G.: Phys. Rev. Lett. **102**, 010401 (2010)
36. Pavičić, M., McKay, B.D., Megill, N.D., Fresl, K.: J. Math. Phys. **51**, 102103 (2010)
37. Gisin, N., Ribordy, G., Tittel, W., Zbinden, H.: Rev. Mod. Phys. **74**, 145 (2002)
38. Coxeter, H.: Regular Polytopes. Dover, New York (1973). Images of several different three-dimensional projections of the 600-cell can be viewed at the following website maintained by David Richter: http://homepages.wmich.edu/~drichter/
39. Aravind, P.K., Lee-Elkin, F.: J. Phys. A **31**, 9829 (1998)